Effects of Pentagone on the Robustness of Dpp Signaling in *Drosophila* Wing Imaginal Disc

MCBU Participants: Brian Nguyen (Graduate: Biology) & Phay Vong (Undergraduate: Mathematics)
MCBU Faculty Advisor: Frederic Y.M. Wan
MCBU Graduate Student Tutor: Cynthia Sanchez-Tapia

Abstract

In early stage of biological development, cells receive positional information from morphogens. One example is the Decapentaplegic (Dpp) signaling process in *Drosophila* wing disc. In this process, Dpp binds to signaling receptors such as Thickvein to form signaling spatial gradients. However, Dpp signaling processes contain many feedback mechanisms that contribute to the overall robustness. For instance, the synthesis rate of the morphogen decapentaplegic (Dpp) in a Drosophila wing imaginal disc has been found to double with an increase of 5.9°C in ambient temperature. To compensate for this change, flies are known to develop normally after such an exogenous change, in some cases accompanied by a wing disc size reduction. Mathematical modeling, analysis and numerical simulations that size reduction in fact could result in size-normalized robustness. This provides a theoretical basis for the observed robust wing development preserving relative but not absolute tissue pattern, when the morphogen synthesis rate is significantly altered. Moreover, Pentagone (Pent) has been suggested to have a negative feedback in the Dpp signaling process. In this project, we investigate how a negative feedback could provides a mechanism for stimulating the size adjustment needed to compensate for the higher Dpp synthesis rate to result in size-normalized robustness.

1.1 Introduction

Morphogens play a critical role in determining the fate of cells and patterning of biological tissues during the early developmental stages of the organism [3]. These cell fates are known to be determined by the concentration gradients of morphogen-receptor complexes. One highly studied morphogen is the *Drosophila* homolog decapentaplegic (Dpp) which is involved in almost all aspects of fly development [2]. Extensive research on *Drosophila* Dpp pathway has provided valuable insight on related processes in vertebrates.

To begin studying cell signaling processes, one area of major interest is the robustness of the *Drosophila* wing disc during early development. Dpp has been known to play a role in patterning and

growth of the wing disc. Many models were developed to explain the role of the Dpp gradient during wing development but, these models are hotly debated. For instance, one model suggested that both Dpp concentration and signaling gradients scale with tissue size during development [7]. Extensive research has been taken to understand the adaptability of the Dpp gradients and one target is the mediator protein Pentagone (Pent). Using the expansion-repression model, it was predicted that the Dpp gradient expansion was Pent-dependent [1]. Overall, the model proposed by Wartlick et al. [7] suggests that cell proliferation is determined by temporal increases of Dpp gradients.

However, new insights can still be obtained about the robustness of Dpp gradient in the *Drosophila* wing imaginal disc. A spatially two-dimensional reaction-diffusion system of partial differential equations (PDE) was developed to study the compensatory effect of the Dpp gradient under environmental pressures [3]. It was discovered that Dpp synthesis rate doubled when the ambient temperature increased by 5.9˚C yet, the fly maintained its relative tissue pattern. Overall, the work provides the theoretical basis to quantify the sensitivity of the fruit fly wing disc to any perturbations [3].

With this model, we aim to understand the feedback regulator Pent on the robustness of Dpp signaling in the *Drosophila* wing imaginal disc. Given the systems of equations from the previous work done by Lander et. al., we set out to account for the effects of Pent by adding a parameter $\kappa(R_b)$to the two-dimensional reaction-diffusion system of PDE.

2.1 The Problem

The morphogen Dpp bind to signaling receptors by the chemical reaction:

$$[\mathrm{L}] + [\mathrm{R}] \underset{\mathrm{k_{off}}}{\overset{\mathrm{k_{on}}}{\rightleftharpoons}} [\mathrm{LR}] \xrightarrow{\mathrm{k_{deg}}} [\mathrm{R}] \qquad (1)$$

Even though the synthesis rate doubles every 5.9 degrees Celsius, the relative wing disc morphogen gradient shape stays the same and the wing disc had normal growth [3]. This property of the morphogen gradient is called robustness. However, the feedback mechanism behind robustness in the

Drosophila wing disc is unknown. The problem we want to solve now is how Pent affects the robustness of Dpp signaling in the wing disc of the Drosophila.

With robustness and Pent, growth will just continue and reach a steady state. Each time, it accommodates for external changes in the environment, then the end shape will change. Therefore the wing span of the Drosophila will change each time and we no longer have a fixed boundary problem. We will have to figure out a way to fix this part of the problem. This also means that we don't know when the robustness checks to see if accommodation is needed. In this paper we are going to see what the effects of Pent are when there is only one accommodation and it is in steady state.

2.2 The Idea

Although the mechanism behind robustness is unknown, we can begin unraveling the mystery by studying the feedback mechanism on Pent. Simplifying the problem, we are going to find what the effects of Pent are near steady state conditions and analyze if the robustness of the Dpp gradient is altered with this new feedback.

To study the feedback mechanism on Pent, we started with the unaccounted Pent reaction-diffusion model of PDE from a previous work on Dpp gradient [3]:

$$\frac{\partial[L]}{\partial T} = D(\frac{\partial^2[L]}{\partial X^2} + \frac{\partial^2[L]}{\partial Z^2}) - k_{on}[L][R] + k_{off}[LR] + V_L(X,Z,T) \quad (2)$$

$$\frac{\partial[LR]}{\partial T} = k_{on}[L][R] - (k_{off} + k_{deg})[LR] \quad (3)$$

$$\frac{\partial[R]}{\partial T} = V_R(X,Z,T) - k_{on}[L][R] + k_{off}[LR] - k_R[R] \quad (4)$$

These equations govern the rate of change of free Dpp [*L(X,Z,T)*], bounded Dpp-Tkv receptor [*LR(X,Z,T)*] and unbounded Tkv receptor [*R(X,Z,T)*] at time *T* and position (*X*,*Z*). The k_{on}, k_{off} and k_{deg} are known as the binding rate constant, the dissociation rate constant and the degradation rate constant, respectively. $D(\frac{\partial^2[L]}{\partial X^2} + \frac{\partial^2[L]}{\partial Z^2})$ represents the diffusion of Dpp throughout the domain *(X,Z)*. Lastly, $V_L(X,Z,T)$ and $V_R(X,Z,T)$ are the synthesis rate of Dpp morphogen and Tkv receptor, respectively. Similar

to the Lander et. al., we are focused on a time-invariant morphogen and receptor synthesis which means that $V_L(X,Z,T) = V_L(X,Z)$ and $V_R(X,Z,T) = V_R(X,Z)$.

As for the boundary conditions, the X- and Z-axis are taken to be in the antero-posterior direction and the apical-proximal direction, respectively [3]. In the antero-posterior, $-X_{min}$ is defined as the midpoint of the Dpp production region yielding:

$$X = -X_{min} : \frac{\partial[L]}{\partial X} = 0 \qquad (5)$$

for $T > 0$ and $0 < Z < Z_{max}$. At the far end or X_{max}, the posterior end is taken to be as a sink:

$$X = X_{max} : [L] = 0 \qquad (6)$$

for $T > 0$ and $0 < Z < Z_{max}$. In the apical-proximal direction, we have a sealed wall at the apical face:

$$Z = 0 : \frac{\partial[L]}{\partial Z} = 0 \qquad (7)$$

for $T > 0$ and $-X_{min} > X > X_{max}$. The proximal direction shows the leakage of free morphogens as indicated by this equation:

$$Z = Z_{max} : \frac{\partial a}{\partial Z} + \frac{\gamma_z}{Z_{max}} a = 0 \qquad (8)$$

for $T > 0$ and $-X_{min} > X > X_{max}$. γ is a dimensionless constant and is our leakage parameter.

At initial conditions $T = 0$, we have the initial conditions [3]:

$$[L] = [R] = 0, [R] = R_0(X, Z) \qquad (9)$$

for $-X_{min} \leq X \leq X_{max}$ and $0 \leq Z \leq Z_{max}$.

With these equations and boundary conditions, we introduce a robustness index (R_b) in terms of [LR] by root mean square differential and a parameter kappa ($\kappa(R_b)$) that adjusts according to the effect of Pent. Once we have the new boundary conditions and equations, we will set the system at steady state conditions and solve these equations for the variable that represents the synthesized Dpp and Thickvein receptor (Tkv). The amount of Dpp [L] and Tkv [R] will also be in terms of the synthesized Dpp and Tkv.

We will end up with an equation all in terms of [L] that will give us a partial differential equation in terms of [L].

According to Lander et. al., the system of equations (2)-(4) can be proven that the solution exists and is unique. We observe solving the equation means that we can find the steady state solution of [L] and therefore we can find the steady state solution of [LR]. We need this because we need the spatial value of [L] for every point on the wing. This will give us our gradient. Once we know the value of [LR], we know the value of the robustness index and therefore the effects of Pent in comparison to normal growth and how it affects the morphogen gradient.

2.3 Methods: Normalization, reparameterization and accounting for Pent

We took the proposed robustness index (R_b) from Vargas, [3]:

$$R_b = \frac{1}{b_h}\sqrt{\frac{1}{l_m}\int_0^{l_m}[b_e(x,0) - b_w(x,0)]^2 dx} \qquad (10)$$

And to account for Pent, a new parameter κ is considered in terms of $\bar{b}$ at steady state with b representing the concentration of [LR], or signaling gradient. $b_w$is the wild type growth, meaning normal growth. $b_e$is the ectopic type growth, one that grows under the environmental changes.

$$\kappa = \frac{1}{1 + c\bar{R}_b^n} \qquad (11)$$

As stated before, the values X_{max}, X_{min}, and Z_{max} change because of the effects of Pent on the robustness, we must have equations for them. Where $\bar{X}_{min}, \bar{Z}_{min}, \bar{X}_{max}$, and$\bar{Z}_{max}$ are the regular growth solutions without the effects of Pent.

$$X_{max} = \kappa\bar{X}_{max} \qquad (12)$$
$$X_{min} = \kappa\bar{X}_{min} \qquad (13)$$
$$Z_{max} = \kappa\bar{Z}_{max} \qquad (14)$$
$$Z_{min} = \kappa\bar{Z}_{min} \qquad (15)$$

We now have to deal with the issue that the boundary is not fixed and will move. To do this we will introduce our new variables x and z, along with our normalizations and reparametrizations to be the following:

$$x = \frac{X}{\kappa \bar{X}_{max}} \tag{16}$$

$$z = \frac{Z}{\kappa \bar{Z}_{max}} \tag{17}$$

$$t = \frac{D}{\bar{Z}_{max}^2} T \tag{18}$$

$$v_L, v_R = \frac{\bar{Z}_{max}^2}{D\bar{R}_0} V_L, V_R \tag{19}$$

$$f_z, g_z, g_r, h_z = \frac{\bar{Z}_{max}^2}{D} k_{off}, kdeg, k_R, k_{on}\bar{R}_0 \tag{20}$$

$$a, b, r, r_0 = \frac{1}{\bar{R}_0}[L], [LR], [R], R_0 \tag{21}$$

Now our boundaries are no longer moving. The new boundaries are the following:

$$x_{max} = l_M \tag{22}$$

$$x_{min} = -x_m \tag{23}$$

$$z_{max} = 1 \tag{24}$$

$$z_{min} = 0 \tag{25}$$

Plugging these into the system of equations (2)-(4), the results from this normalization and reparametrization can be found below:

$$\frac{\partial a}{\partial t} = \frac{1}{\kappa^2}\left(\frac{\partial^2 a}{\partial x^2} + \frac{\partial^2 a}{\partial z^2}\right) - h_z a r + f_z b + e v_L(x, z) \tag{26}$$

$$\frac{\partial b}{\partial t} = h_z a r - (f_z + g_z) b \tag{27}$$

$$\frac{\partial r}{\partial t} = v_R(x, z) - h_z a r + f_z b - g_r r \tag{28}$$

A new variable *e* is placed on the $v_L(x,z)$ term because it will help determine the state we are in. If we were normal growth, then its value would be one. If it were 5.9 degrees Celsius hotter, its value would be two. This accommodates for the doubling in Dpp synthesis discussed previously.

The new boundary conditions become:

$$x = -x_m : \frac{\partial a}{\partial x} = 0 \tag{29}$$

$$x = l_M : a = 0 \tag{30}$$

$$z = 0 : \frac{\partial a}{\partial z} = 0 \tag{31}$$

$$z = 1 : \frac{\partial a}{\partial z} + \kappa \gamma_z a = 0 \tag{32}$$

To solve the system of equations, we solved $\underline{r}$ and $\underline{b}$ in terms of $\underline{a}$ at steady state conditions:

$$\bar{r} = \frac{\alpha_z r_0(x)}{\alpha_z + \xi \bar{a}} \qquad \bar{b} = \frac{r_0(x)\bar{a}}{\alpha_z + \xi \bar{a}} \tag{33}$$

$$\xi = \frac{g_z}{g_r} \qquad \alpha_z = \frac{g_z + f_z}{h_z} \tag{34}$$

Plugging these into equation 26 will give us the PDE equation we want to solve at steady state conditions:

$$\frac{1}{\kappa^2}\left(\frac{\partial^2 a}{\partial x^2} + \frac{\partial^2 a}{\partial z^2}\right) - \frac{g_z r_0(x) a}{\alpha_z + \xi \bar{a}} + e v_L H(-x) = 0 \tag{35}$$

Where $v_L(x,z)$ is uniform in z and $v_L(x) = e\kappa^2 \underline{v_z} H(-x)$. It is a step function because at $x=0$, we no longer have Dpp production in the system.

2.4 Linear Case: Low Receptor Occupancy

Finally, we move onto solving the equation. First we solved the linear equation by setting $\xi = 0$ to reflect the case of low receptor occupancy that results from high receptor synthesis rate or low morphogen synthesis rate [3]. This yields a linear equation:

$$\frac{1}{\kappa^2}\left(\frac{\partial^2 a}{\partial x^2} + \frac{\partial^2 a}{\partial z^2}\right) - \frac{g_z \rho^2 a}{\alpha_z} + e v_L H(-x) = 0 \tag{36}$$

The heaviside function makes us solve two equations instead of one. For the first case:

$$\left(\frac{\partial^2 \bar{a}}{\partial x^2} + \frac{\partial^2 \bar{a}}{\partial z^2}\right) - \kappa^2 \frac{g_z \rho^2 \bar{a}}{\alpha_z} = 0 \tag{37}$$

We used the technique of eigenfunction expansion because we saw that it was solvable using separation of variables, by letting $\bar{a} = \Phi(x)\Psi(z)$. Our two differential equations came out to be,

$$\frac{\partial^2 \phi(\bar{x})}{\partial x^2} = \mu^2 \phi(\bar{x}) \tag{38}$$

$$\frac{\partial^2 \psi(\bar{z})}{\partial z^2} = -l^2 \psi(\bar{z}) \tag{39}$$

where we chose l^2 to be an arbitrary constant and $\mu^2 = l^2 + \kappa^2 \, g_z/\alpha_z$. The solutions are ones we are familiar with. The first equation would be the exponential solution and the second is a function of sine and cosines. We can reduce the number of coefficients by using boundary conditions. This is yet to be done.

$$\bar{a}(x,z) = (C_1 e^{\bar{x}\mu} + C_2 e^{-\bar{x}\mu})(C_3 sin(lz) + C_4 cos(lz)) \tag{40}$$

To solve the second equation, in the range where $v_L(x) = e\kappa^2 \bar{v}_z$, we can't see a clear and easy solution.

$$(\frac{\partial^2 \bar{a}}{\partial x^2} + \frac{\partial^2 \bar{a}}{\partial z^2}) - \kappa^2 \frac{g_z \rho^2 \bar{a}}{\alpha_z} + e\kappa^2 \bar{v}_z = 0 \tag{41}$$

Let's assume that $\bar{a}$ and $v_L(x)$ was an infinite series of cosine.

$$a = \sum_{n=0}^{\infty} A_n(x) cos(\lambda_n z) \tag{42}$$

$$v_L(x) = \sum_{n=1}^{\infty} v_n \bar{v}_z cos(\lambda_n z) \tag{43}$$

Where $\lambda_n$and $v_n$are unknown coefficients to the series. We found that the solution for $\bar{a}$ was:

$$\bar{a}(x,z) = \sum_{n=1}^{\infty} \frac{v_n \bar{v}_z \kappa^2}{\beta} (1 - \frac{cosh(\beta_n l_M)}{cosh(\beta_n (l_M + x_m))} cosh(\beta_n (x + x_m))) cos(\lambda_n z) \tag{44}$$

Now that we have a proposed solution, now we need to make sure the function value and its derivative to be continuous at *x=0* of the both solutions we found. This is yet to be done.

2.5 Algorithm

For the solution to the non-linear case, we are going to solve it numerically and validate it with our analytical solution from the low receptor occupancy case. For the non-linear case, we are solving the equation when $\xi > 0$, shown below:

$$\nabla^2 a = \kappa^2 \frac{g_z a}{\alpha_z + \xi a} - \kappa^2 e v_L H(-x) \qquad (45)$$

Finite differences and a *Newton like* method were used to find the numerical solution of the robust signaling gradient. The coding scheme was written in MATLAB. With finite differences method, the numerical scheme of equation (45) has the form:

$$Ma = h^2 f(a) \qquad (46)$$

where *M* is the matrix for the Laplacian operator, *h* is the step size and *f(a)* the right hand side of equation (45). Using the finite differences method, we generated a matrix of the Laplacian operator by modifying the matrix that utilizes the Dirichlet boundary conditions [4] and the following boundary conditions were used to modify the NxN matrix, illustrated below:

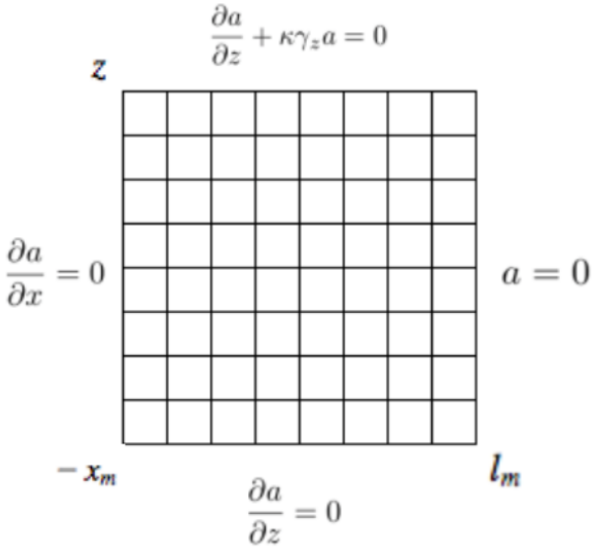

To obtain the solution to *a,*we used the *Newton like* method which consist of three algorithms called the Damped Newton, Inexact Newton and Jacobi-free Newton [5], illustrated below:

Damped Newton
Algorithm: $a = update(a_{old}, e)$
s = 1; $r_{old} = ||f(a_{old}) - Ma_{old}||$; $r = r_{old} + 1$;
while $r > r_{old}$
$a = a_{old} + s * e$;
$r = ||f(a) - Ma||$;
$s = s/2$;
end

This algorithm is our residual equation and updates our solution a until it reaches convergence indicated by the residual error (r). We set the tolerance to be 10^{-5} and s is a simple bisection scheme to aid our search direction δa[5]. To solve our residual equation, we need to solve e by the Inexact Newton method:

Inexact Newton
Algorithm: e = inexact(J, r, θ)
$e_0 = 0$; $r_{in} = ||r||$;
while $||r_{in}|| > \theta||r||$
$e = e + Jr$;
$r_{in} = r - J * e$;
end

The Inexact Newton is referred to as the inner iteration to solve the Jacobian equation $Je = r$ and we set $\theta = 0.6$ [5]. With these algorithms, we input them into our Jacobian-free Newton method:

Jacobian-free Newton
Algorithm: a = NewtonMethod(tol,k,e)
$a = 0$; $r_0 = f(0)$; $r = r_0$;
while $||r||/||r_0|| \geq tol$
$r = ||f(a) - Ma||$;
$J = Ma - f'(a)$;
$e = inexact(J, r, \theta)$;
$a_{old} = a$;
$a = update(a_{old}, e)$;
end

With our initial solution to a when $R_b = 0$, we used the value to solve for the wild-type Dpp signaling gradient (b_w), indicated by the equation (33) where $r_0(x) = 1, \xi = 1$ and $\alpha = 0.0201$. However, to solve for the ectopic signaling gradient (b_e), it requires the convergence of R_b according to our coding scheme, below:

Robust Index Convergence

while | R_b - R_{b_old} | > TolRb
e = 2;
$a_e = NewtonMethod(tol, k, e)$;
$b_e = \frac{a_e}{\alpha+\xi a_e}$;
$R_{b\_old} = R_b$;
$R_b = (\frac{1}{b_h}) * \sqrt{(\frac{1}{l_m}) * (b_e(x,0) - b_w(x,0))^2}$;
k =
update(R_b);
end

function k = update(R_{b_old})
c = 1;
k = 1/(1+c*R_{b_old});
end

If the difference between the new R_b and R_{b_old} was higher than the tolerance (TolRb) of 10^{-5}, then the code would start a new iteration. In the new iteration, the new R_b will be used to find a new solution $a_{ectopic}$which will be used to find the b_e.

3.1 Results

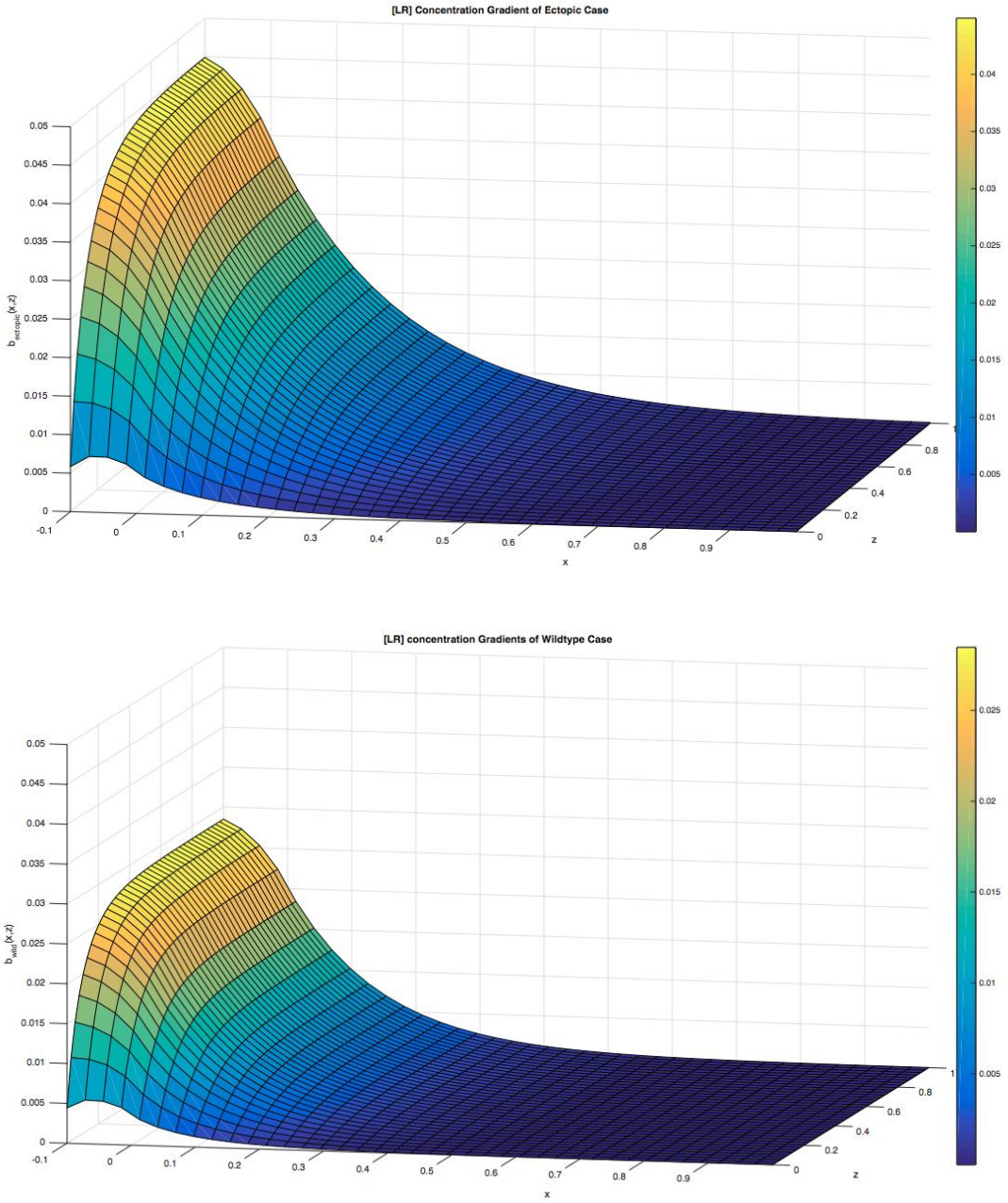

Fig 1. (a) This is the ectopic type at steady state conditions with parameters $\xi = 1, v_z = 0.05, \& \alpha = 0.0201$.The R_b values is 0.3475 while κ value is 0.7421. **(b)** This is the Dpp gradient of the wild type at near steady state conditions with $R_b = 0$ and $\kappa = 1$.

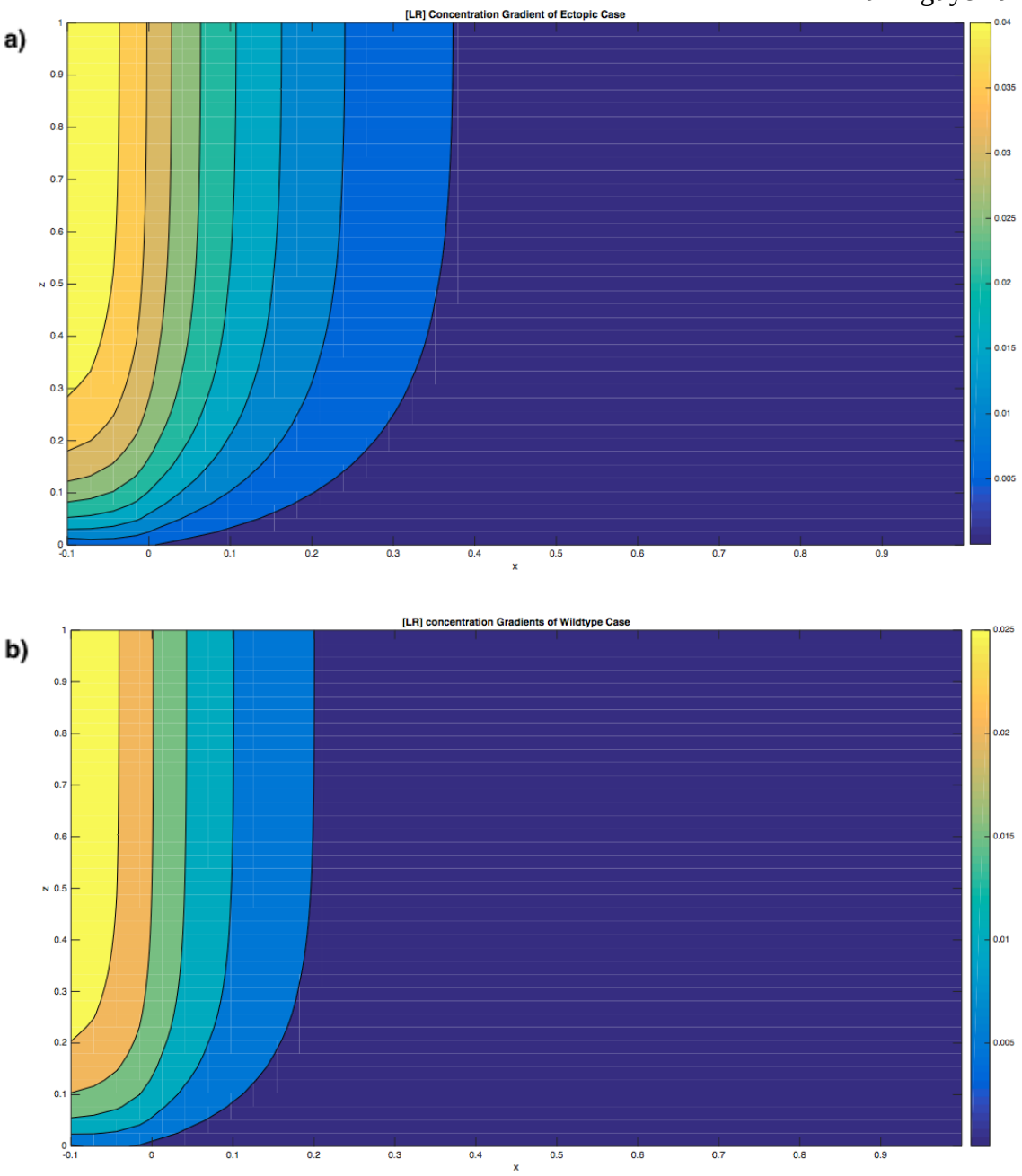

Fig 2. (a) & (b) These are the contour plots for the ectopic and wild-type, respectively. The size of signaling gradients for ectopic and wild-type are different.

4.1 Related Works

The work done by Lander et. al. on the robustness of Dpp gradient in *Drosophila* wing disc was the foundation of our investigation about the effect of Pent on robustness. Their study provided the theoretical basis for the observed robustness of wing development when discovering that the *Drosophila*

wing disc preserved its relative tissue pattern when the ambient temperature increased by 5.9˚C which doubled the Dpp synthesis rate [3]. However, the model does not account for the effects of Pent which is suggested to play a role in Dpp signaling [1]. To study Pent, we added a new parameter $\kappa(R_b)$to the model from Lander et. al. and analyzed the effects. We hope that by gathering basic information about the effects of Pent on Dpp signaling in the *Drosophila* wing disc, it may encourage new experimental research on Pent.

Moreover, we recognize that our model may not be biologically realistic in describing the changes of the Dpp gradient shape with the effect of Pent. Living cells have the capability to continuously sense, transmit, and process internal and external perturbations [7]. By only observing robustness near steady state condition, our system may be responding too slow.

5.1 Conclusion and Further Work

By understanding the effect of Pent, we can add in more possibilities that may either helps or hinders the robustness of the Dpp signaling in *Drosophila* wing disc. From Fig 1, we observed that the morphogen gradient shapes from both the wild type and ectopic cases are slightly different in size.

To validate the non-linear solution, we plan to solve for the low occupancy receptor case, or the linear case. This is a special biological case in which the system has a low Dpp synthesis rate or high Tkv receptor synthesis [3]. While solving the linear case, we found the solution to be an infinite series of cosine and exponentials. Since there was a heaviside function, this made us solve two equations. The next step is to match the limits of the two equations at x = 0.

Lastly, we plan to study the effects of Pent when the model system is not at steady state conditions. This requires modifying κ by incorporating a Hill function in order to account for the tolerance level of the model system. By working on these, we hope to gain further insights on the robustness of Dpp signaling in *Drosophila* fruit wing disc.

6.1 Acknowledgement

We are grateful for the support by the National Science Foundation UBM grant DMS-1129008, the University of California, Irvine, and the MCBU Summer Research program to allow us to conduct this research. We are also thankful for our faculty research advisor Dr. Wan and graduate mentor Cynthia Sanchez-Tapia. It was their tireless and nurturing efforts that helped us grow as researchers.

References

1. Ben-Zvi, D.; Pyrowolakis, G.; Barkai, N.; Shilo B-Z. Expansion-Repression Mechanism for Scaling the Dpp Activation Gradient in Drosophila Wing Imaginal Discs. Current Biology. 2011, 21, 1391-1396.
2. Hamaratoglu, F.; Affolter, M.; Pyrowolakis, G. Dpp/BMP signaling in flies: From molecules to biology. Elsevier. 2014, 32, 128-136.
3. Lander, A.D.; Nie, Q.; Vargas, B.; Wan, F.Y.M. Size-Normalized Robustness of Dpp Gradient in Drosophila Wing Imaginal Disc. J. Mechanics of Materials and Structures. 2011, 6, 1-4.
4. Long, C. Finite Difference Methods. http://www.math.uci.edu/~chenlong/226/FDM.pdf.
5. Long, C. Iterative Methods for Nonlinear Elliptic Equations. 2011. http://www.math.uci.edu/~chenlong/226/NonlinearEllipticPDE.pdf
6. Steuer, R.; Waldherr, S.; Sourjik, V.; Kollmann, M. Robust Signal Processing in Living Cells. PLOS. 2011. DOI: 10.1371/journal.pcbi.1002218.
7. Wartlick, O.; Mumcu, P.; Kicheva, A.; Bittig, T.; Seum, C.; Jülicher, F.; González-Gaitán, M. Dynamics of Dpp Signaling and Proliferation Control. Science. 2012, 331, 1154-1161.